

Aberystwyth University

Inducible glutathione S-transferase (IrgST1) from the tick Ixodes ricinus is a haem-binding protein

Perner, Jan; Kotál, Jan; Hatalová , Tereza; Urbanová , Veronika; Bartošová-Sojková, Pavla; Brophy, Peter; Kopáek, Petr

Published in:

Insect Biochemistry and Molecular Biology

DOI:

[10.1016/j.ibmb.2018.02.002](https://doi.org/10.1016/j.ibmb.2018.02.002)

Publication date:

2018

Citation for published version (APA):

Perner, J., Kotál, J., Hatalová , T., Urbanová , V., Bartošová-Sojková, P., Brophy, P., & Kopáek, P. (2018). Inducible glutathione S-transferase (*IrgST1*) from the tick *Ixodes ricinus* is a haem-binding protein. *Insect Biochemistry and Molecular Biology*, 95, 44-54. <https://doi.org/10.1016/j.ibmb.2018.02.002>

General rights

Copyright and moral rights for the publications made accessible in the Aberystwyth Research Portal (the Institutional Repository) are retained by the authors and/or other copyright owners and it is a condition of accessing publications that users recognise and abide by the legal requirements associated with these rights.

- Users may download and print one copy of any publication from the Aberystwyth Research Portal for the purpose of private study or research.
- You may not further distribute the material or use it for any profit-making activity or commercial gain
- You may freely distribute the URL identifying the publication in the Aberystwyth Research Portal

Take down policy

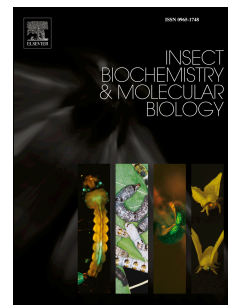
If you believe that this document breaches copyright please contact us providing details, and we will remove access to the work immediately and investigate your claim.

tel: +44 1970 62 2400
email: is@aber.ac.uk

Accepted Manuscript

Inducible glutathione S-transferase (*IrGST1*) from the tick *Ixodes ricinus* is a haem-binding protein

Jan Perner, Jan Kotál, Tereza Hatalová, Veronika Urbanová, Pavla Bartošová-Sojtková, Peter M. Brophy, Petr Kopáček



PII: S0965-1748(18)30021-3

DOI: [10.1016/j.ibmb.2018.02.002](https://doi.org/10.1016/j.ibmb.2018.02.002)

Reference: IB 3035

To appear in: *Insect Biochemistry and Molecular Biology*

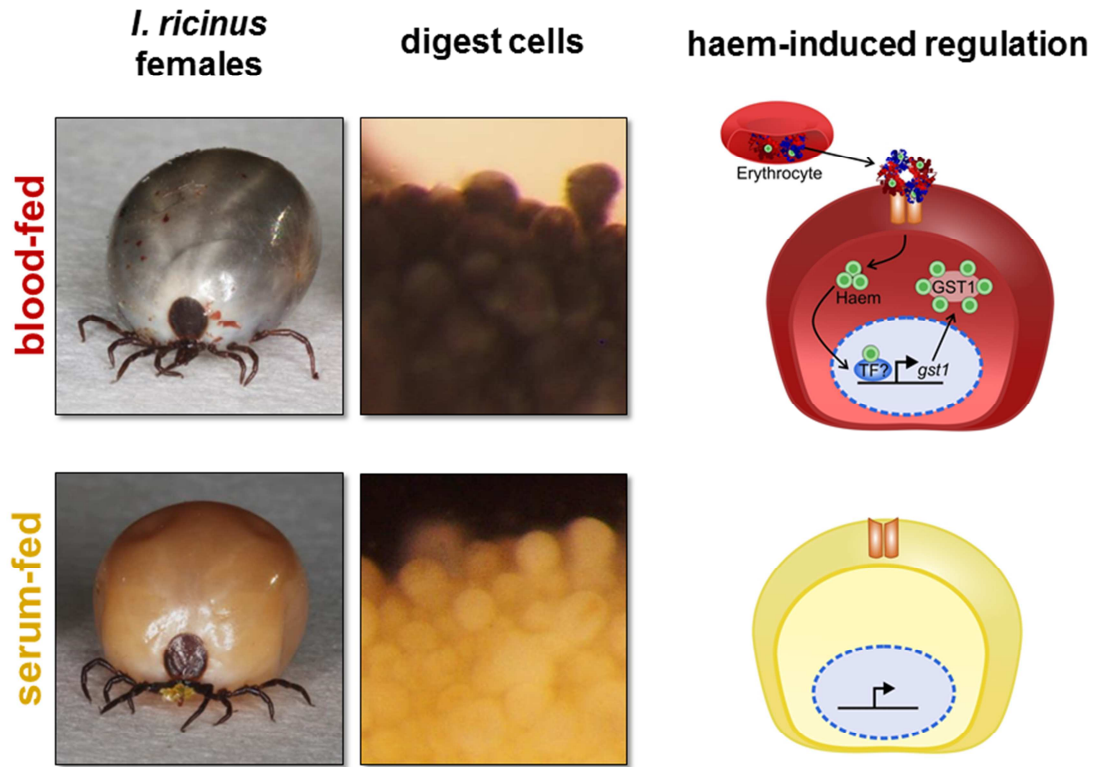
Received Date: 19 January 2018

Revised Date: 14 February 2018

Accepted Date: 19 February 2018

Please cite this article as: Perner, J., Kotál, J., Hatalová, T., Urbanová, V., Bartošová-Sojtková, P., Brophy, P.M., Kopáček, P., Inducible glutathione S-transferase (*IrGST1*) from the tick *Ixodes ricinus* is a haem-binding protein, *Insect Biochemistry and Molecular Biology* (2018), doi: 10.1016/j.ibmb.2018.02.002.

This is a PDF file of an unedited manuscript that has been accepted for publication. As a service to our customers we are providing this early version of the manuscript. The manuscript will undergo copyediting, typesetting, and review of the resulting proof before it is published in its final form. Please note that during the production process errors may be discovered which could affect the content, and all legal disclaimers that apply to the journal pertain.



ACCEPTED MANUSCRIPT

1 **Inducible glutathione S-transferase (*IrGST1*) from the tick *Ixodes ricinus* is a**
2 **haem-binding protein**

3 Jan Perner^{a,b*}, Jan Kotál^{a,b}, Tereza Hatalová^b, Veronika Urbanová^a, Pavla Bartošová-
4 Sojková^a, Peter M. Brophy^c, Petr Kopáček^a

5 ^a Institute of Parasitology, Biology Centre of the Czech Academy of Sciences, Branišovská 31, 370 05,
6 České Budějovice, Czech Republic

7 ^b Faculty of Science, University of South Bohemia, Branišovská 31, 370 05, České Budějovice, Czech
8 Republic

9 ^c Institute of Biological, Environmental and Rural Sciences (IBERS), Aberystwyth University, Aberystwyth,
10 SY23 3DA, UK

11
12 **Abstract**

13 Blood-feeding parasites are inadvertently exposed to high doses of potentially cytotoxic haem liberated
14 upon host blood digestion. Detoxification of free haem is a special challenge for ticks, which digest
15 haemoglobin intracellularly. Ticks lack a haem catabolic mechanism, mediated by haem oxygenase, and
16 need to dispose of vast majority of acquired haem *via* its accumulation in haemosomes. The knowledge of
17 individual molecules involved in the maintenance of haem homeostasis in ticks is still rather limited.
18 RNA-seq analyses of the *Ixodes ricinus* midguts from blood- and serum-fed females identified an
19 abundant transcript of *glutathione S-transferase (gst)* to be substantially up-regulated in the presence of
20 red blood cells in the diet. Here, we have determined the full sequence of this encoding gene, *ir-gst1*, and
21 found that it is homologous to the delta-/epsilon-class of GSTs. Phylogenetic analyses across related
22 chelicerates revealed that only one clear *IrGST1* orthologue could be found in each available
23 transcriptome from hard and soft ticks. These orthologues create a well-supported clade clearly separated
24 from other ticks' or mites' delta-/epsilon-class GSTs and most likely evolved as an adaptation to tick
25 blood-feeding life style. We have confirmed that *IrGST1* expression is induced by dietary haem(oglobin),
26 and not by iron or other components of host blood. Kinetic properties of recombinant *IrGST1* were
27 evaluated by model and natural GST substrates. The enzyme was also shown to bind haemin *in vitro* as
28 evidenced by inhibition assay, VIS spectrophotometry, gel filtration, and affinity chromatography. In the
29 native state, *IrGST1* forms a dimer which further polymerises upon binding of excessive amount of
30 haemin molecules. Due to susceptibility of ticks to haem as a signalling molecule, we speculate that the
31 expression of *IrGST1* in tick midgut functions as intracellular buffer of labile haem pool to ameliorate its
32 cytotoxic effects upon haemoglobin intracellular hydrolysis.

33

34 1. Introduction

35 Ticks are blood-feeding ectoparasites notorious for transmitting a wide variety of infection diseases of
36 humans as well as farm and companion animals (de la Fuente et al., 2008). Hard ticks (Ixodidae) undergo
37 a life cycle of three parasitic stages - larvae, nymphs, and adults, each of which requires one blood meal as
38 the only source of nutrients for their further development and reproduction. Adult hard tick females
39 imbibe large quantities of host blood exceeding up to hundred times their unfed weight. The blood meal is
40 ultimately processed into the huge clutch of eggs before the female dies (Sonenshine and Roe, 2014). The
41 proteinaceous components of the blood meal are internalised by tick digest cells lining up the midgut
42 epithelium. The host proteins are then hydrolysed intracellularly, in the endo-lysosomal system consisting
43 of a network of acidic cysteine and aspartic peptidases (Sojka et al., 2013). Haemoglobin degradation is
44 inevitably concomitant with the intracellular release of haem, a pro-oxidative molecule, which is
45 potentially cytotoxic when in excess (Graca-Souza et al., 2006).

46 We have recently demonstrated that ticks lost genes encoding enzymes involved in both haem
47 biosynthesis and haem degradation (Perner et al., 2016a). Instead, ticks acquire haem exogenously, from
48 the host haemoglobin (Perner et al., 2016a). A small portion of acquired haem is further dispatched for
49 systemic inter-tissue distribution to allow assembly of endogenous haemoproteins, while most of the haem
50 has to be disposed by effective means of detoxification. In contrast to haemozoin formation, a well-
51 described mechanism of haem disposal in malaric plasmodium, schistosomes, or rhodnius vectors, ticks
52 accumulate excessive haem as non-crystalline aggregates, in a specialised organelles generally referred to
53 as haemosomes (Lara et al., 2005; Lara et al., 2003). Haem intracellular transport from digestive vesicles
54 to cytosol was reported to be mediated by an ATP-binding cassette (ABCB10) (Lara et al., 2015).
55 However, the next fate of cytosolic haem is still poorly understood.

56 In order to contribute to the knowledge of haem metabolism in ticks, we have tested, by RNA-seq
57 analyses, which transcripts change their levels in response to the presence of red blood cells (RBCs) in the
58 tick diet. For this purpose, we compared the transcriptomes of midguts from *I. ricinus* females membrane-
59 fed either bovine blood or bovine serum. Among the surprisingly low number of transcripts with
60 decreased or elevated levels in response to RBCs presence, we identified a gut-specific transcript Ir-
61 114935 encoding a delta-/epsilon-class glutathione S-transferase (Perner et al., 2016b).

62 Members of the glutathione S-transferases (GSTs) family are ubiquitously present in eukaryotic organisms
63 where they serve mainly in cellular detoxification of endogenous or xenobiotic compounds *via* their
64 conjugation with the reduced glutathione (GSH), which results in their increased water solubility and
65 excretion (Townsend and Tew, 2003; Wilce and Parker, 1994). Based on their organismal origin, primary
66 sequence, substrate specificity, immunological, or chromosomal localisations, the GSTs can be grouped
67 into more than a dozen classes historically tagged by Greek letters (Mashiyama et al., 2014). The

68 availability of the tick *Ixodes scapularis* genome (Gulia-Nuss et al., 2016) made it possible to enumerate
69 and classify GSTs encoded in this species (Reddy et al., 2011). Out of 35 identified *IsGST* genes, 32
70 encoded cytosolic GSTs comprising 14 genes of vertebrate/mammalian Mu-class, 7 genes of Delta- and 5
71 genes of Epsilon- classes specific for insects, and 3 genes each were of common Omega- and Zeta- classes
72 (Reddy et al., 2011). Given their capability to detoxify xenobiotics, GSTs have a well-established role in
73 development of insecticide resistance in insect pests (for review see e.g. (Enayati et al., 2005) or acaricide
74 resistance in ticks (Dreher-Lesnick et al., 2006; Duscher et al., 2014; He et al., 1999; Vaz et al., 2004a)).
75 However, much less is known about the house-keeping physiological function of GSTs in the management
76 of potentially toxic endogenous haem originating from the blood meal diet of the haematophagous
77 parasites.

78 In this work, we provide a biochemical and functional characterisation of the haem(oglobin)-inducible
79 GST from *I. ricinus* (further referred to as *IrGST1*) and demonstrate that this enzyme is capable to
80 efficiently bind haemin *in vitro*. Clear orthologues of *IrGST1* could be found only in other tick species,
81 but not in other organisms, suggesting that *IrGST1* represents a novel class of tick-specific GSTs that
82 evolved during the adaptation of ticks to their blood-feeding life style.

83

84 2. Materials and methods

85 2.1. Tick maintenance and natural feeding

86 Adult *I. ricinus* ticks were collected in the forest near České Budějovice. Ticks were kept at 24 °C and
87 95% humidity under a 15:9-hour day/night regime. All laboratory animals were treated in accordance with
88 the Animal Protection Law of the Czech Republic No. 246/1992 Sb., ethics approval No. 357 095/2012.
89 The study was approved by the Institute of Parasitology, Biology Centre of the Czech Academy of
90 Sciences (CAS) and Central Committee for Animal Welfare, Czech Republic (protocol no. 1/2015).

91

92 2.2. Tick membrane feeding

93 Membrane feeding of ticks was performed using a stationary six-well plate format according to Thomas
94 Kröber and Patrick Guerin (Kröber and Guerin, 2007). Whole bovine blood was collected in a local
95 slaughter house and manually defibrinated. To obtain serum, whole blood samples were centrifuged at
96 $2500 \times g$, 10 min, 4°C and the resulting supernatant was collected and centrifuged again at $10\,000 \times g$,
97 10 min, 4°C. Fifteen females were placed in a feeding unit lined with a thin (80–120 µm) silicone
98 membrane, previously pre-treated with a bovine hair extract in dichloromethane (0.5 mg of low volatile
99 lipids). After 24 hr, unattached or dead females were removed and an equal number of males were added
100 to the attached females into the feeding unit. Diets were exchanged in a 12h regime, with concomitant

101 addition of 1 mM adenosine triphosphate (ATP) and gentamicin (5 μ g/ml). For diet supplementation, pure
102 bovine haemoglobin (Sigma - H2500), bovine holo-Transferrin (Rocky Mountain Biologicals), and
103 haemin (Sigma - H9039) was used. For membrane feeding experiments, haemin stock solution (62.5 mM
104 haemin dissolved in 100 mM NaOH), was diluted 100 \times to reach 625 μ M (final concentration) equalling a
105 haem equimolarity with 1% haemoglobin (w/v).

106
107 *2.3. Tissue dissection, RNA extraction, cDNA synthesis, and RT-qPCR*
108 Membrane-fed *I. ricinus* females were forcibly removed from the membrane on day 6 of feeding. Tick
109 midguts were dissected on a paraplast-filled Petri dish under a drop of ice-cold DEPC-treated PBS. Total
110 RNA was isolated from dissected tissues using a NucleoSpinRNA II kit (Macherey-Nagel, Germany),
111 quality checked by gel electrophoresis on agarose gel, and stored at -80 $^{\circ}$ C prior to cDNA synthesis. cDNA
112 preparations were made from 0.5 μ g of total RNA in independent triplicates using the Transcriptor High-
113 Fidelity cDNA Synthesis Kit (Roche Diagnostics, Germany). The cDNA served as templates for
114 subsequent quantitative expression analyses by RT-qPCR. Samples were analysed by a LightCycler 480
115 (Roche) using Fast Start Universal SYBR Green Master Kit (Roche). Relative expressions were calculated
116 using the $\Delta\Delta$ Ct method (Pfaffl, 2001). The expression profiles were normalised to *I. ricinus* elongation
117 factor 1 α (*ef-1 α*). List of primers is available as Supplementary Table S1.

118
119 *2.4. Sequencing, cloning, and phylogenetic analysis of IrGST1*
120 Full cDNA sequence of gene encoding *IrGST1* was amplified using primers derived from 5'- and 3'-
121 untranslated regions of the orthologous *I. scapularis* gene (ISCW005803) (Supplementary Table S1). *I.*
122 *ricinus* midgut-specific cDNA prepared from midguts of females fed for 3 days served as template. The
123 amplified 786 bp long PCR product was cloned into a pCR4-TOPO TA vector (Invitrogen) and
124 sequenced. Amino acid sequences of *IrGST1* and other selected delta-/epsilon-class GSTs were aligned
125 using the E-INS-i algorithm in MAFFT v7.017 (Katoh et al., 2002) and manually trimmed in Geneious
126 v8.1.3. (Kearse et al., 2012) to the final length of 221 amino acids. Maximum parsimony analysis was
127 performed in PAUP* v4.b10 (Swofford, 2003) using a heuristic search with random taxa addition, the
128 ACCTRAN option, TBR swapping algorithm, all characters treated as unordered and gaps treated as
129 missing data. Maximum-likelihood analysis was performed in RAxMLv7.2.8 (Stamatakis, 2006) under the
130 PROTGAMMABLOSUM62 + Γ model. Mosquitoes *Anopheles gambiae* and *Aedes aegypti* were used as
131 outgroups. Bootstraps were based on 1000 replicates for both analyses. Bayesian inference analysis was
132 performed in MrBayes v3.0 (Ronquist and Huelsenbeck, 2003) using the WAG + Γ model of evolution.
133 Analyses were initiated with random starting trees, four simultaneous MCMC chains sampled at intervals
134 of 200 trees and posterior probabilities estimated from 1 million generations (burn-in 100 000).

135 2.5. Expression and purification of recombinant polyhistidine-tagged and untagged *IrGST1*

136 Poly-histidine tagged recombinant *IrGST1* was prepared by amplification of a coding sequence using *ir-*
137 *gst1*-specific primers (Supplementary Table S1) and the 694 bp product was cloned into a pet100 vector
138 (Invitrogen) following manufacturers' protocol. Resulting plasmid was transformed into TOP10 *E. coli*
139 cells and positive clones were selected on ampicillin LB plates, sequenced, and transformed into *E. coli*
140 BL21 Star (DE3) chemically competent cells (Invitrogen). Cells were grown in ampicillin LB medium at
141 37°C and when reached OD = 1.6, the culture was induced with 0.1 mM isopropyl β -D-1-
142 thiogalactopyranoside (IPTG). The cells were cultured for 6 h and the harvested cells were suspended in
143 PBS and homogenised using sonication. The centrifuged homogenate was loaded on a Ni²⁺-IMAC agarose
144 (GE Healthcare) and the resin was washed with 20 bed volumes of 20 mM phosphate buffer pH 6.0, 0.5 M
145 NaCl, 20 mM imidazol, 10% glycerol and 0.5% Triton X-100 (v/v) to remove non-specifically bound
146 proteins. The recombinant protein was then eluted from the resin by 100 mM imidazole in a washing
147 buffer, concentrated and transferred to the PBS by ultrafiltration using 15 ml centrifuge filter units (cut-off
148 10 kDa, Merck Millipore). The monospecific polyclonal antibodies against *IrGST1* were raised in rabbits
149 as previously described (Grunclova et al., 2006) and used for Western blotting. A PCR product encoding
150 an untagged recombinant *IrGST1* was amplified using the same primer pair (with the reverse primer
151 containing a stop codon), cloned into the pet101 vector (Invitrogen), and further expressed in *E. coli* as
152 described above. The cell pellet was homogenised in a tenth of original culture volume in 20 mM Tris pH
153 8.5 and centrifuged at 10 000 \times g, 20 min, 4°C. The supernatant was filtered through a 0.22 μ m filter
154 (Merck Millipore) and applied on MonoQ HR 5/5 column (GE Healthcare) using an AKTA pure
155 chromatographic system (GE Healthcare). The sample was separated at 1 ml/min flowrate in 20 mM Tris
156 pH 8.5 and eluted by a 0–500 mM NaCl gradient. The fractions with enriched GST activity (see below)
157 were pooled, concentrated by ultrafiltration (10 kDa cut-off), applied onto Superdex 75 10/300 GL
158 column (GE Healthcare) and further separated at 1 ml/min flowrate in 20 mM Tris pH 8.5, 150 mM NaCl.
159 Gel filtration molecular standards (ferritin, aldolase, serum albumin, and chymotrypsinogen A) were used
160 for molecular weight determination. Purified *IrGST1* was used for immunising mice and the mice immune
161 sera were used for immunohistochemistry (see below).

162

163 2.6. Reducing SDS-PAGE and Western blot analysis

164 Tick midgut homogenates were prepared in 1% Triton X-100 in PBS supplemented with a Complete™
165 cocktail of protease inhibitors (Roche) using a 29G syringe needle, and subsequently subjected to three
166 freeze/thaw cycles using liquid nitrogen. Proteins were then extracted for 1 hr at 4°C and 1 200 rpm using
167 a Thermomixer comfort (Eppendorf, Germany). Samples were then centrifuged 15 000 \times g, 10 min, 4°C
168 and separated by reducing SDS-PAGE on 12.5 % polyacrylamide gels. Protein profiles were visualized

169 using TGX stain-free chemistry (BioRad) or by staining with Coomassie Brilliant Blue R-250 (CBB).
170 Proteins were transferred onto Immun-Blot® LF PVDF membrane using a Trans-Blot Turbo system
171 (BioRad). For Western blot analyses, membranes were blocked in 3% (w/v) non-fat skimmed milk in PBS
172 with 0.05% Tween 20 (PBS-T), incubated in immune serum ($\alpha IrGST1$) diluted in PBS-T (1:5000) or in
173 immune serum against *I. ricinus* ferritin 1 ($\alpha IrFer1$) diluted in PBS-T (1:50). The goat anti-rabbit IgG-
174 peroxidase antibody (Sigma A9169) diluted in PBS-T (1:50000) was used as a secondary antibody.
175 Signals were detected using ClarityWestern ECL substrate, visualized using a ChemiDoc MP imager, and
176 analysed using Image Lab Software (BioRad).

177

178 2.7. Substrate specificities of *IrGST1* and isoelectric focusing

179 The substrate specificities of *IrGST1* were tested with known model and natural substrates of GSTs
180 (Morphew et al., 2012). In brief, enzyme assays were measured using a UV/VIS Gilford Response
181 spectrophotometer over 3 min at 25°C. Glutathione S-transferase (GST) activity was determined using the
182 model substrate 1-chloro-2,4-dinitrobenzene (CDNB) according to the method described by Habig et al.
183 (Habig et al., 1974). The enzyme assay was performed in 100 mM potassium phosphate buffer pH 6.5,
184 containing 1mM reduced glutathione (GSH) and 1mM CDNB at 340 nm ($\epsilon = 9.6 \times 10^6 \text{ cm}^{-2} \text{ mol}^{-1}$). GSH-
185 dependent peroxidase activity of *IrGST1* was determined using cumene hydroperoxide (the model lipid
186 hydroperoxide substrate)(Jaffe and Lambert, 1986). The assay was carried out in 50 mM phosphate buffer
187 pH 7.0 containing 1 mM GSH, 0.2 mM NADPH, 0.5 U glutathione reductase (Sigma, G3664), and 1.2
188 mM cumene hydroperoxide. The reaction was measured at 340 nm ($\epsilon = 6.22 \times 10^6 \text{ cm}^{-2} \text{ mol}^{-1}$). GST
189 activity with trans-2-nonenal was determined as previously described (Brophy et al., 1989) The reaction
190 mix was composed of 100 mM potassium phosphate buffer pH 6.5, 1 mM GSH, and 0.23 mM trans-2-
191 nonenal and the enzymatic activity was measured at 225 nm ($\epsilon = -19.2 \times 10^6 \text{ cm}^{-2} \text{ mol}^{-1}$). Isoelectric
192 focusing (IEF) was performed on IEF precast gels (BioRad) and separated by IEF cathode buffer 2mM
193 lysine (free base), 2 mM arginine (free base) and IEF anode buffer 0.7 mM phosphoric acid at increased
194 voltage modes: 100 V 60 min, 250 V 60 min, 500 V 30 min. IEF markers of pI range 3–10 were used
195 (SERVA 39212.01).

196

197 2.8. Determination of kinetic parameters and inhibition studies

198 The determination of *IrGST1* apparent Michaelis constants to CDNB and GSH as substrates were
199 performed in triplicates, with varying concentrations of CDNB and constant GSH (1 mM), or constant
200 CDNB (1 mM) and varying concentrations of GSH, respectively. Kinetic constants were calculated by
201 non-linear regression analysis of the experimentally measured activities. Data were fitted to the Michaelis-
202 Menten equation using GraphPad Prism 6.0 software. The inhibition of *IrGST1* by haem-related

203 compounds was investigated by CDNB activity assay with haemin (haem-chloride), haematin (haem-
204 hydroxide, Sigma H3281), protoporphyrin IX (PPIX) (Sigma P8293), and myoglobin (Sigma M0630).
205 Haemin and haematin were dissolved in 100 mM NaOH, PPIX in DMSO, and myoglobin in H₂O.

206

207 2.9. Examination of haemin-*IrGST1* binding by spectrophotometry and haemin-affinity chromatography

208 The absorption properties of haemin in the presence of *IrGST1* were measured by recording the
209 absorption spectra in the range from 300 nm to 450 nm using a UV-1800 spectrophotometer (Shimadzu).
210 Constant concentration of haemin (10 µM) in 20 mM sodium phosphate buffer (pH 8.0), 50 mM NaCl
211 was incubated for 15 min with different concentrations of *IrGST1* corresponding to the molar ratios of r-
212 *IrGST1*: haemin from 0 to 2.

213 Binding of *IrGST1* to the commercial haemin-agarose (Sigma H6390) was examined using a pull down
214 experiment. *E. coli* expressing *IrGST1* (see above) were homogenised in 1.5 ml of 50 mM Tris-HCl pH
215 8.0, 0.5 M NaCl (Tris-NaCl buffer), centrifuged and the supernatant was incubated with 50 µl of haemin-
216 agarose for 1 h with slow rotation. Agarose beads were then allowed to settle, supernatant removed, and
217 the agarose was then transferred to an empty column (BioRad) and extensively washed with Tris-NaCl
218 buffer. Specifically bound proteins were then eluted with 1 M urea in Tris-NaCl buffer and separated
219 using SDS-PAGE. Coomassie-stained protein band was excised and prepared for mass fingerprint
220 analysis. Briefly, the excised gel was incubated with 50 mM ammonium bicarbonate: 100% acetonitrile
221 (1:1) solution for 15 minutes at 37°C to destain the gel. The gel was dehydrated in 100% acetonitrile for
222 30 minutes at 37°C and subsequently rehydrated in trypsin solution (100 ng/µl) in ammonium bicarbonate,
223 left for 45 minutes at 8°C, and incubated at 37°C over-night. Supernatant was removed and the gel was
224 washed several times alternately with acetonitrile and 50 mM ammonium bicarbonate. Samples were then
225 vacuum-dried, resuspended 1% formic acid (w/w) and analysed by LC MS/MS on an Agilent 6550
226 iFunnel Q-TOF mass spectrometer with a Dual AJS ESI source coupled to a 1290 series HPLC system
227 (Agilent, Cheshire, UK) according to Morpew et al. 2014 (Morpew et al., 2014).

228

229 2.10. Haemin binding size exclusion chromatography

230 Haemin binding size exclusion chromatography was performed with *IrGST1*, diluted to 35 µM (0.9
231 mg/ml) in 20 mM Tris pH 8.5, 150 mM NaCl. Different molar ratios of haemin (stock solution 35 mM
232 haemin in 100 mM NaOH) were added to 1 ml of *IrGST1* solution and incubated for 30 minutes, 250 rpm,
233 22°C in ThermoMixer® (Eppendorf). Then 250 µl of the membrane filtered (0.22 µm) incubation reaction
234 was separated using Superdex 75 10/300 GL column (GE Healthcare) at 1 ml/min flow rate in 20 mM Tris
235 pH 8.5, 150 mM NaCl and the absorbance was monitored at the dual wavelengths of 280 and 400 nm.

236

237 2.11. RNA interference and immunohistochemistry

238 dsRNA of *ir-gst1* or *gfp* (green fluorescent protein) used for control were synthesised using the
239 MEGAscript T7 transcription kit (Ambion, Lithuania) according to the previously described protocol
240 (Hajdušek et al., 2009). *I. ricinus* females were injected into the haemocoel through to the coxae with *ir-*
241 *gst1*-specific dsRNA or control *gfp* dsRNA (0.5 µl; 3 µg/µl) using a microinjector (Narishige), allowed to
242 rest for one day and then fed naturally for 5 days on guinea pigs. The efficiency of RNA-mediated
243 silencing *ir-gst1* gene expression was verified at the protein level by Western blot analysis using $\alpha IrGST1$
244 antibodies. The visualisation of authentic *IrGST1* by indirect immune-fluorescent microscopy in the
245 dissected *I. ricinus* guts was performed as described earlier (Franta et al., 2010) with some modification.
246 Briefly, the semi-thin sections were cut, transferred onto glass slides, and blocked with 1% BSA and 10%
247 goat serum PBS-T (0.3% Triton X-100) for 1 h. Incubation with the primary $\alpha IrGST1$ antibody (1:100) in
248 PBS-T was performed in a humid chamber for 1.5 h at room temperature. For negative control
249 experiments, the primary antibody incubation was omitted (not shown). Sections were washed with PBS-T
250 (four times 5 min) and then incubated with Alexa Fluor[®] 488 secondary dye-conjugated goat anti-mouse
251 (Invitrogen/Molecular Probes) diluted to 1:500 in PBS-T for 1 h at room temperature. After washing with
252 PBS-T, the slides were counterstained with DAPI (4',6'-diamidino-2-phenylindole; 2.5 µg/ml; Sigma) for
253 5 min. Finally, sections were mounted in Fluoromount (Sigma-Aldrich) and examined using the
254 fluorescence microscope BX 53. The semi-thin sections stained with toulidine blue were examined under
255 the light mode of the microscope BX53. The same protocol was carried out for immunodetection of 4-
256 hydroxynonenal (4-HNE) using the commercial rabbit α 4-HNE antibody (Abcam ab46545, 1:300) and the
257 1:500 diluted Alexa Fluor[®] 488-labeled secondary goat anti-rabbit antibody (Invitrogen/Molecular
258 Probes).

259
260

261 3. Results

262 3.1. *IrGST1* sequence identification and phylogenetic analysis

263 The transcript Ir-114935, previously shown to be significantly up-regulated in the midguts of blood-fed
264 compared to serum-fed ticks (Perner et al., 2016b), encodes a partial sequence of a putative delta-/epsilon-
265 class glutathione S-transferase. The partial sequence was clearly orthologous to *I. scapularis*
266 ISCW005803 gene encoding delta-class GST, *IsGSTD2* (Reddy et al., 2011), with 98% sequence identity
267 at both amino-acid and nucleotide levels. The full coding sequence of *IrGST1* (deposited in the GenBank
268 under Access. No. MF984398) was obtained by cloning and sequencing of a 786 bp long PCR product
269 amplified using the primers derived from 5'- and 3'-UTR regions of *I. scapularis IsGSTD2*. All
270 performed phylogenetic analyses have unambiguously revealed the *IrGST1* orthologues of delta-/epsilon-

271 class from other hard and soft tick species that create a well-supported clade (Fig. 1A). This specific clade
272 is distinct from the clades of other delta-/epsilon- class GSTs from *I. scapularis*, horseshoe crab, and mites
273 (Fig. 1A), which display much lower sequence identity to *IrGST1* (below 50%) (Fig. 1B and
274 Supplementary Fig. S1). The typical SNAIL/TRAIL signature motif present in GSTs of various classes is
275 conserved within the *IrGST1* orthologous group as SRAI(A/G). All ticks and mites delta-/epsilon-class
276 GSTs possess a conserved tyrosine residue at the position 6 (Fig. 1B and Supplementary Fig. S1)
277 classifying the enzymes into Y-type major subgroup of cytosolic GSTs (Atkinson and Babbitt, 2009).

278

279 3.2. Expression of *IrGST1* in the tick gut is inducible by haemin

280 Even though we have previously demonstrated by RNA-seq and qRT-PCR that expression of contig Ir-
281 114935 encoding *IrGST1* is up-regulated in ticks fed on the whole blood (Perner et al., 2016b), a question
282 remaining to be solved was which constituent of red blood cells is responsible for the up-regulation of the
283 *ir-gst1* gene. In order to reveal that, we have conducted a membrane feeding experiment where the ticks
284 were allowed to feed for 5 days haemoglobin-free serum, haemoglobin-free serum supplemented either
285 with 1% w/v bovine haemoglobin, 625 μ M haemin (haemin solubilised in sodium hydroxide), mock
286 (sodium hydroxide, 1 mM final concentration), whole blood reconstituted with red blood cells. RT-qPCR
287 analysis revealed that *ir-gst1* is up-regulated by dietary haemin as well as by haemoglobin (Fig. 2A). The
288 up-regulation was observed higher for dietary haemin (unbound or secondarily complexed with albumin)
289 compared to dietary haemoglobin, when the concentration of haem were equimolar. The consistent result
290 was obtained at the protein level, as evidenced by Western blot analysis (Fig. 2B). The levels of *IrGST1* in
291 the midgut were dose-dependent on the amount of haemin added to the serum diet and gradually increased
292 from micromolar dietary concentration to 625 μ M representing about 1/150 of the physiological
293 concentration of haem present in the whole blood (~ 10 mM) (Fig. 2C). This result indicates that *IrGST1*
294 inducibility by host haem may serve as a very sensitive sensor of the blood meal uptake. To confirm that
295 *IrGST1* expression is induced exclusively by haem and not by iron, we performed a membrane feeding
296 experiment where ticks were fed diets enriched with bovine holo-transferrin and bovine haemoglobin,
297 known tick sources of iron and haem, respectively (Perner et al., 2016a). We confirmed that while ticks
298 fed transferrin-enriched diet had elevated levels of *IrFer1*, *IrGST1* levels remained unaltered. Conversely,
299 ticks fed haemoglobin enriched diet had elevated levels of *IrGST1* and unaltered levels of *IrFer1* (Fig.
300 2D). These results underscore that haem and iron sensing in the tick midgut are independent processes.

301

302 3.3. RNAi effectively silences the expression of *IrGST1* throughout the tick feeding

303 To study a physiological role of *IrGST1* *in vivo*, a knock-down of this transcript was obtained by RNAi-
304 mediated silencing. A confirmation of clear down-regulation of *IrGST1* in tick midgut throughout the

305 feeding was evidenced by Western Blotting (Fig. 3A). Indirect immune-fluorescence microscopy using
306 *α IrGST1* antibody confirmed a substantial decrease of fluorescent signal in the matured midgut digest
307 cells of *IrGST1*-KD females compared to the control ticks injected with *gfp* dsRNA (Fig. 3B). However,
308 this reduction of *IrGST1* in tick midgut digest cells had no obvious impact on the tick feeding and
309 fecundity. *IrGST1*-KD females could accomplish feeding, reached comparable engorged weights, laid egg
310 clutches of comparable size and colour that gave rise to viable larvae similarly as the control *gfp* group
311 (Fig. 3C, D). GSTs are also known to conjugate GSH to 4-hydroxynonenal (4-HNE), that is a toxic
312 product of lipid peroxidation and a biomarker of oxidative stress (Awasthi et al., 2004; Cheng et al.,
313 2001). The presence of 4-HNE inside the digest cells was detected by indirect immune-fluorescent
314 microscopy. However, no difference of fluorescent intensity was observed in guts from *IrGST1*-KD and
315 control females (Supplementary Fig. S2), suggesting that *IrGST1* is not involved in 4-HNE detoxification.
316 Given the absence of any *IrGST1*-KD phenotype, we further focused on *in vitro* characterisation of
317 recombinant *IrGST1*.

318

319 3.4. Preparation and enzymatic characterisation of recombinant *IrGST1*

320 Recombinant *IrGST1* was first expressed in *E. coli* expression system as a His-tagged protein with a
321 theoretical mass 29721 Da and purified in a soluble form from the bacterial lysate using Ni²⁺-IMAC
322 chromatography under native conditions (Fig. 4A). *E. coli* expressed *IrGST1* was active in GSH
323 transferase activity assay using a model substrate 1-chloro-2,4-dinitrobenzene (CDNB) (Fig. 4B). The
324 crude extract of *E. coli* cells had a specific enzymatic activity of 201 ± 13 nmol CDNB/min/mg protein
325 that following elution and dialysis increased to 1820 ± 77 nmol CDNB/min/mg protein in the purified
326 fraction with Km for GSH to be 0.87 ± 0.13 mmol and Km for CDNB to be 2.9 ± 0.64 mmol
327 (Supplementary Fig S3). Despite the capacity to utilise GSH in a CDNB activity assay (Km values for
328 GSH and CDNB were comparable to other reported GSTs (Al-Qattan et al., 2016)), the effort to purify
329 *IrGST1* from *E. coli* crude extract or further purify the *IrGST1* (IMAC purified) using GSH- or S-hexyl
330 GSH-Sepharose failed given the low binding affinity to these sorbents (Supplementary Fig. S3).
331 GSTs display a wide range of enzymatic activities with model substrates (Brophy et al., 1990). To reveal
332 the kinetic parameters of *IrGST1*, assays with typical GST substrates were also carried out using another
333 invertebrate recombinant GST (*Fasciola gigantica* sigma GST) as a control (Morphew et al., 2012).
334 Beside the above mentioned GSH-conjugating activity using CDNB as a model substrate, the *IrGST1*
335 exerted also peroxidase activity with the model lipid hydroperoxide substrate - cumene hydroperoxide
336 (Fig. 4B). *IrGST1* had no activity towards reactive carbonyls, in contrast to sigma-class *F. gigantica*, GST
337 as assayed using trans-2-nonenal as a natural substrate derived from lipid peroxidation (Brophy et al.,
338 1989) (Fig. 4B).

339 As several GSTs from different blood feeding parasites have been reported to bind haemin (see below), we
340 have performed a haemin interaction/inhibitory assay of *IrGST1* GSH-conjugating activity and compared
341 it to the *FgGST* over a range of CDNB substrate concentration (Fig. 4C). This experiment revealed that
342 *IrGST1* activity is much more sensitive to haemin than *FgGST*. In order to determine more precisely the
343 inhibition constant of haemin (K_i) for *IrGST1*, a Dixon plot of inhibitory activities was used and K_i of
344 haemin was determined to be 42 ± 15 nM, indicating a strong binding affinity for *IrGST1* (Fig. 4D). Using
345 the CDNB activity assay, we further examined whether free haem, protein-bound haem, or iron-free
346 protoporphyrin IX (PPIX) is responsible for the inhibition of *IrGST1*. Both free haemin (haem-chloride)
347 and haematin (haem-hydroxide) inhibited the *IrGST1* activity with apparent IC_{50} around 200 nM, whereas
348 myoglobin-bound haem or iron-free protoporphyrin IX (PPIX) did not induce any inhibition at the
349 concentration range up to 1 μ M (Fig. 4E).

350

351 3.5. Recombinant *IrGST1* binds haemin in vitro

352 To further support evidence of haemin binding to the *IrGST1*, crude extract from *E. coli* expressing
353 *IrGST1* was incubated with haemin-agarose in a pull down assay. Roughly 75 % of *E. coli* extract proteins
354 remained unbound in the supernatant, whereas the CDNB-specific activity was virtually lost (Fig. 5A),
355 likely confined to the haemin-agarose pellet. After extensive washing with 20 mM phosphate buffer pH
356 7.4, 0.5 M NaCl, haemin-bound proteins were eluted with washing buffer supplemented with 1 M urea.
357 SDS-PAGE analysis showed a major protein band of about 29 kDa (Fig. 5A), which was submitted to the
358 peptide mass-fingerprint analysis that confirmed its identity as *IrGST1* with about 19% sequence
359 coverage. To further elucidate the binding characteristics of haemin to *IrGST1*, we evaluated the binding
360 properties by spectrophotometry at visible wavelength range. Unbound haemin displays an absorption
361 maximum at $\lambda = 385$ nm, but its absorption maximum undergoes intensifying red-shifts upon binding to
362 *IrGST1*, with isobestic point at $\lambda = 402$ nm, in the titration experiment where the *IrGST1* was treated as a
363 ligand and haemin concentration was kept constant at 10 μ M (Fig. 5B). The point of saturation on the
364 monitoring wavelength ($\lambda = 421$ nm) was reached at 1:1 molar ratio (Fig. 5C), indicating that one *IrGST1*
365 molecule binds one molecule of haemin.

366

367 3.6. Native *IrGST1* is a haemin-binding dimer

368 In order to rule out a possible contribution of protein poly-histidine tag to haemin binding, untagged
369 recombinant *IrGST1* was expressed in *E. coli* system and purified using two-step liquid chromatography
370 by anion exchange chromatography (IEX) on the MonoQ column followed by size exclusion
371 chromatography (SEC) on a Superdex 75 column (Fig. 6A). Monitoring absorbance at both $\lambda = 280$ nm
372 and $\lambda = 400$ nm, revealed that the purified *IrGST1* already displayed some basal absorbance at 400 nm,

373 indicating that *IrGST1* strips endogenous haem from expressing *E. coli* cells (Fig. 6B). The molecular
374 weight of the *IrGST1* was determined by SEC using calibration standards and calculated to be of 56.7 kDa
375 implying a dimeric form (Fig. 6B). Isoelectric point of the native *IrGST1*, determined experimentally by
376 isoelectric focusing, was pI 5.5 (Supplemental Fig. S4). To assess the molecular arrangement of the
377 *IrGST1* - haemin complex, the *IrGST1* was titrated with different molar concentrations of haemin and the
378 products were analysed by SEC. As shown in the Fig. 6C, *IrGST1* has the capacity to bind haemin as a
379 dimer. When haemin is in excess, up to eight to one molar ratios to *IrGST1*, a fraction of the protein shifts
380 towards higher molecular weights suggesting further polymerisation or aggregation of the *IrGST1*-haemin
381 complex (Supplementary Fig. S5).

382

383 4. Discussion

384 The glutathione S-transferases (GSTs) from pathogens that carry out disposal of toxic endogenous and
385 exogenous compounds have been investigated as potential targets for development of efficient anti-
386 parasitic drugs and vaccines for three decades (Brophy et al., 1990; Harwaldt et al., 2002; Nare et al.,
387 1992; Ricciardi and Ndao, 2015; Wei et al., 2016; Zhan et al., 2005; Zhan et al., 2010).

388 In this work, we have characterised a novel haem-inducible GST from the hard tick *I. ricinus* (*IrGST1*),
389 which transcript was markedly up-regulated in blood-fed ticks compared to ticks fed with serum (Perner et
390 al., 2016b). *IrGST1* belongs to the delta-/epsilon-class (insect type) GSTs and only one clear orthologue
391 could be found among other 32 cytosolic GSTs identified in the genome of a closely relative species *I.*
392 *scapularis* (Reddy et al., 2011). Accordingly, only one transcript orthologous to *IrGST1* could be found in
393 transcriptomes available for other tick species. One haem-responsive GST, namely GST-19 (CE09995)
394 has been identified using a proteomic approach among 36 nu-class members annotated in the genome of
395 the model nematode *Caenorhabditis elegans* (Perally et al., 2008). Twenty six genes encoding GSTs were
396 annotated in the mosquito *Aedes aegypti*, out of which the gene *gstx2* (new, unclassified class) showed an
397 affinity for haematin (Lumjuan et al., 2007). Lately, a substantial up-regulation of this gene transcript was
398 demonstrated using a transcriptome-wide analysis of haem influence on *A. aegypti* cell line (Bottino-Rojas
399 et al., 2015).

400 Our phylogenetic analyses grouping haem-binding *IrGST1* with just one orthologue in each tick species
401 (Fig. 1A, B) suggests that this tick-specific group likely exapted from an ancestral catalytic GST to form
402 haem-binding GSTs under the evolution pressure exerted by their blood-feeding life style. This is
403 supported by a distant phylogenetic positioning of tick putative haem-binding GSTs from other delta-
404 /epsilon-class GSTs present in related non-haematophagous chelicerates (horseshoe crab and mites).

405 Several GSTs that have been at least partially characterised in ticks so far belong mostly to the mu-class
406 (see (Shahein et al., 2013) for review). The first tick GST was purified from the larval stage of the cattle

407 tick *Rhipicephalus (Boophilus) microplus* using glutathione affinity chromatography (He et al., 1999). A
408 gene encoding another mu-class GST from *R. microplus* (referred to as *BmGST*) was isolated from
409 salivary gland cDNA library, and its tissue and developmental stage profiling revealed that *bm-gst* gene is
410 transcribed in salivary glands and midguts of the adult females but not in the larval stage (Rosa de Lima et
411 al., 2002). The enzyme kinetic parameters of the recombinant *BmGST* using the CDNB assay were
412 determined together with the inhibitory potential for a number of compounds present in commercial
413 acaricides (Vaz et al., 2004a). Two mu-class GSTs were cloned from the tick *Haemaphysalis longicornis*
414 (*HIGST*) and *Rhipicephalus appendiculatus* (*RaGST*). The recombinant enzymes were reported to be
415 effectively inhibited by acaricides, especially ethion and deltamethrin (Vaz et al., 2004b). Given the cross-
416 reactivity of antibodies raised against recombinant *HIGST* from *H. longicornis* with *BmGST* from *R.*
417 *microplus*, the cattle immunized with *HIGST* were partially protected against infestation by the cattle ticks
418 (Parizi et al., 2011) that implies tick GSTs as a candidate antigen for anti-tick vaccine development (de la
419 Fuente et al., 2016). Most recently, the vaccination potential of *HIGST* was tested against rabbit
420 infestation with two closely related species *R. appendiculatus* and *R. sanguineus*. Despite the close
421 similarity of GSTs from these tick species, the partial protection was obtained only against adult *R.*
422 *appendiculatus* females (vaccine efficacy was reported to be of about 67%), but no protection was
423 achieved against any stage of *R. sanguineus* (Sabadin et al., 2017). Another mu-class GST (tagged as
424 *BaGST*) was cloned from the Egyptian cattle tick *R. (B.) annulatus* and the active recombinant *BaGST*
425 was expressed and purified as fusion protein His-tagged protein (Shahein et al., 2008). This GST was later
426 shown to be effectively inhibited by phenolic compounds and flavonoids from plant extracts but also by a
427 haematin (Guneidy et al., 2014). RNAi-mediated silencing of the GST from *R. sanguineus* revealed the
428 role of this enzyme in permethrin detoxification as the GST-KD ticks were more susceptible to the
429 acaricide exposure (Duscher et al., 2014). The only partially characterised tick delta-/epsilon-class GST
430 member was the *DvGST1* from *Dermacentor variabilis* (Fig. 1). The gene encoding *DvGST1* was
431 reported to be specifically expressed in the tick gut and up-regulated by blood feeding (Dreher-Lesnack et
432 al., 2006), which is suggestive to have a similar function as *IrGST1*.
433 *Ir-gst1* expression is tissue-specific for *I. ricinus* midgut (Perner et al., 2016b), where it is localised to the
434 cytosol of the digest cell (Fig. 3B). Its mRNA and protein levels are markedly up-regulated by addition of
435 a soluble haemin into the diet. The inducibility is more sensitive for soluble haemin rather than for haem
436 bound as a prosthetic group of haemoglobin (Fig. 2). This might indicate that free haemin is taken up by
437 the digest cells by an alternative route independently of the proposed haemoglobin-specific receptor
438 mediated uptake, potentially disbalancing intracellular haem homeostasis (Lara et al., 2005; Sojka et al.,
439 2013). Importantly, haem sensing in the tick midgut is independent of iron sensing in the tissue, as
440 *IrGST1* expression is induced only by dietary haem, and not by dietary iron (Fig. 2D). Unlike the iron

441 homeostasis, which is controlled at the translational level by proteosynthesis of intracellular iron storage
442 protein - ferritin 1 (Hajdušek et al., 2009; Kopacek et al., 2003; Perner et al., 2016a), haem-inducible
443 expression of *IrGST1* is apparently controlled at the level of gene transcription. In mammals, inducible
444 GSTs are known to be regulated through antioxidant response element by the Keap1-Nrf2 pathway
445 (Kansanen et al., 2013). Although several Nrf2-related transcripts containing basic leucine zipper (bZIP)
446 domain have been found to be present in the *I. ricinus* midgut transcriptome (Perner et al., 2016b), their
447 possible role as haem-responsive transcription factor(s) remains to be investigated.

448 Beside the *ir-gst1* inducibility by a dietary haem, we found that the GSH-conjugation activity of
449 recombinant *IrGST1* (determined by CDNB assay) is noncompetitively inhibited by soluble haemin but
450 not by iron-free porphyrin ring (protoporphyrinogen IX) or protein-bound haem (myoglobin) (Fig. 4). We
451 further showed that, in the native state, *IrGST1* forms a dimer and binds haem in an equimolar ratio. The
452 K_i of haemin to *IrGST1* was in the mid nanomolar range, comparable to the inhibition constants reported
453 earlier for GSTs from other hematophagous parasites (Torres-Rivera and Landa, 2008). Haem-binding
454 properties were investigated for several nematode-specific nu-class GSTs from different hookworm
455 species such as *Haemonchus contortus*, *Ancylostoma caninum*, *Necator americanus*, or *Ancylostoma*
456 *ceylanicum* (van Rossum et al., 2004; Wei et al., 2016; Zhan et al., 2005; Zhan et al., 2010). Recombinant
457 *Na-GST1* from *N. americanus* elicited a significant reduction of hookworm burdens in vaccinated
458 hamsters and hereby it became a leading vaccine candidate to prevent human hookworm infections (Zhan
459 et al., 2010). Several haem-binding GSTs were also characterised in flatworms such as the sigma-class
460 GSTs from flukes *Fasciola hepatica* (Brophy et al., 1990) or *FgGST-S1* from *F. gigantica* (Morphew et
461 al., 2012). Much attention has been paid also to the haem-binding GSTs from different *Schistosoma* sp.
462 (Walker et al., 1993) especially for their potential as promising vaccine candidates against human or
463 bovine schistosomiasis (Capron et al., 2001; Capron et al., 1995; Ricciardi and Ndao, 2015). The most
464 thoroughly investigated haem-binding GST has been *PfGST*, the only cytosolic GST encoded in the
465 genome of the malaria parasite *Plasmodium falciparum* (Harwaldt et al., 2002; Liebau et al., 2002). The
466 quite abundant *PfGST*, constituting about 3% of the total extractable proteins, forms in its native state a
467 homodimer (Harwaldt et al., 2002) and was shown to capture haem that failed to be detoxified *via*
468 polymerization in haemozoin (Liebau et al., 2002; Liebau et al., 2005). The 3D molecular structure of
469 *PfGST* was resolved by X-ray diffraction (Fritz-Wolf et al., 2003) that further allowed to perform a
470 molecular docking for a variety of *PfGST* ligands including haemin (Al-Qattan et al., 2016). We have
471 demonstrated, using size exclusion chromatography (Fig. 6 C), that, in its native state, *IrGST1* binds
472 haemin as a dimer at 1:1 molar ratio (Fig. 6 C). Moreover, the *in vitro* experiment showed that *IrGST1*-
473 haemin binding occurs in the absence of reduced glutathione, a feature reported also for the *PfGST*
474 (Liebau et al., 2009). In this work, the authors also described a transition of active *PfGST* dimer to an

475 inactive tetramer. We have observed a similar polymerisation of *IrGST1* in the presence of molar excess
476 of haemin (Supplementary Fig. S5), suggesting that inhibition of *IrGST1* enzyme activity by haemin
477 resulted also in formation of inactive polymer.

478 As mentioned above, several GSTs became a potential target for development of anti-parasitic vaccines
479 (Capron et al., 2001; Capron et al., 1995; Parizi et al., 2011; Ricciardi and Ndao, 2015; Zhan et al., 2010).
480 Although *IrGST1* seems to be the only haem-binding GST expressed in the tick gut, its RNAi-mediated
481 silencing did not result in any clear phenotype impairing tick feeding and further development. Also our
482 pilot vaccination experiments with recombinant *IrGST1* did not elicit any protection of immunised rabbits
483 against tick infestation (data not shown). These findings rather limit the potential of *IrGST1* as a target for
484 anti-tick intervention.

485 Under normal situation, ticks seem to be capable to efficiently detoxify excessive haem *via* its aggregation
486 in haemosomes (Lara et al., 2003). Based on the functional analogy with the *P. falciparum* *PfGST*
487 (Harwaldt et al., 2002; Liebau et al., 2009; Muller, 2015), our biochemical data indicates that *IrGST1*
488 serves as a “back-up” guard molecule, i.e. by mopping up excess haemin and/or neutralising *via* lipid
489 peroxidase activity the downstream consequence of haemin assault on membranes. Thus, *IrGST1* acts as
490 ligandin, when high haemin levels override haemosome capacity and haemin is free in the cytosol and
491 thus harmful to the tick.

492

493 **Acknowledgements**

494 This project was supported by the Czech Science Foundation-grant Nos. 13-11043S and 18-01832S to
495 P.K., by the Czech Academy of Sciences MSM200961802 to J.P, and by the “Centre for research of
496 pathogenicity and virulence of parasites“ (No. CZ.02.1.01/0.0/0.0/16_019/0000759) funded by
497 European Regional Development Fund (ERDF) and Ministry of Education, Youth and Sport (MEYS).
498 The scientific stay of JP in the laboratory of PMB was supported by the project for student
499 internationalisation and development IP 16-1807 from the University of South Bohemia. The authors
500 gratefully acknowledge the assistance of Dr. Rebecca Stuart and Dr. Russ Morphew. We are also
501 grateful to Jan Erhart for excellent technical support and Louise Robbertse for assistance with the
502 graphical abstract.

503

504

505

506

507 **References**

- 508 Al-Qattan, M.N., Mordi, M.N., Mansor, S.M., 2016. Assembly of ligands interaction models for
509 glutathione-S-transferases from *Plasmodium falciparum*, human and mouse using enzyme kinetics
510 and molecular docking. *Comput Biol Chem* 64, 237-249.
- 511 Atkinson, H.J., Babbitt, P.C., 2009. Glutathione transferases are structural and functional outliers in the
512 thioredoxin fold. *Biochemistry* 48, 11108-11116.
- 513 Awasthi, Y.C., Yang, Y., Tiwari, N.K., Patrick, B., Sharma, A., Li, J., Awasthi, S., 2004. Regulation of 4-
514 hydroxynonenal-mediated signaling by glutathione S-transferases. *Free Radic Biol Med* 37, 607-619.
- 515 Bottino-Rojas, V., Talyuli, O.A., Jupatanakul, N., Sim, S., Dimopoulos, G., Venancio, T.M., Bahia, A.C.,
516 Sorgine, M.H., Oliveira, P.L., Paiva-Silva, G.O., 2015. Heme Signaling Impacts Global Gene
517 Expression, Immunity and Dengue Virus Infectivity in *Aedes aegypti*. *PLoS One* 10, e0135985.
- 518 Brophy, P.M., Southan, C., Barrett, J., 1989. Glutathione transferases in the tapeworm *Moniezia expansa*.
519 *Biochem J* 262, 939-946.
- 520 Brophy, P.M., Crowley, P., Barrett, J., 1990. Detoxification reactions of *Fasciola hepatica* cytosolic
521 glutathione transferases. *Molecular and biochemical parasitology* 39, 155-161.
- 522 Capron, A., Riveau, G., Grzych, J.M., Boulanger, D., Capron, M., Pierce, R., 1995. Development of a
523 vaccine strategy against human and bovine schistosomiasis. Background and update. *Mem Inst*
524 *Oswaldo Cruz* 90, 235-240.
- 525 Capron, A., Capron, M., Dombrowicz, D., Riveau, G., 2001. Vaccine strategies against schistosomiasis:
526 from concepts to clinical trials. *Int Arch Allergy Immunol* 124, 9-15.
- 527 Cheng, J.Z., Sharma, R., Yang, Y., Singhal, S.S., Sharma, A., Saini, M.K., Singh, S.V., Zimniak, P., Awasthi, S.,
528 Awasthi, Y.C., 2001. Accelerated metabolism and exclusion of 4-hydroxynonenal through induction
529 of RLIP76 and hGST5.8 is an early adaptive response of cells to heat and oxidative stress. *J Biol Chem*
530 276, 41213-41223.
- 531 de la Fuente, J., Estrada-Pena, A., Venzal, J.M., Kocan, K.M., Sonenshine, D.E., 2008. Overview: Ticks as
532 vectors of pathogens that cause disease in humans and animals. *Front Biosci* 13, 6938-6946.
- 533 de la Fuente, J., Kopacek, P., Lew-Tabor, A., Maritz-Olivier, C., 2016. Strategies for new and improved
534 vaccines against ticks and tick-borne diseases. *Parasite Immunol* 38, 754-769.
- 535 Dreher-Lesnick, S.M., Mulenga, A., Simser, J.A., Azad, A.F., 2006. Differential expression of two
536 glutathione S-transferases identified from the American dog tick, *Dermacentor variabilis*. *Insect*
537 *Molecular Biology* 15, 445-453.
- 538 Duscher, G.G., Galindo, R.C., Tichy, A., Hummel, K., Kocan, K.M., de la Fuente, J., 2014. Glutathione S-
539 transferase affects permethrin detoxification in the brown dog tick, *Rhipicephalus sanguineus*. *Ticks*
540 *Tick Borne Dis* 5, 225-233.
- 541 Enayati, A.A., Ranson, H., Hemingway, J., 2005. Insect glutathione transferases and insecticide resistance.
542 *Insect Molecular Biology* 14, 3-8.
- 543 Franta, Z., Frantova, H., Konvickova, J., Horn, M., Sojka, D., Mares, M., Kopacek, P., 2010. Dynamics of
544 digestive proteolytic system during blood feeding of the hard tick *Ixodes ricinus*. *Parasit Vectors* 3,
545 119.
- 546 Fritz-Wolf, K., Becker, A., Rahlfs, S., Harwaldt, P., Schirmer, R.H., Kabsch, W., Becker, K., 2003. X-ray
547 structure of glutathione S-transferase from the malarial parasite *Plasmodium falciparum*. *Proc Natl*
548 *Acad Sci U S A* 100, 13821-13826.
- 549 Graca-Souza, A.V., Maya-Monteiro, C., Paiva-Silva, G.O., Braz, G.R., Paes, M.C., Sorgine, M.H., Oliveira,
550 M.F., Oliveira, P.L., 2006. Adaptations against heme toxicity in blood-feeding arthropods. *Insect*
551 *Biochem Mol Biol* 36, 322-335.

- 552 Grunclova, L., Horn, M., Vancova, M., Sojka, D., Franta, Z., Mares, M., Kopacek, P., 2006. Two secreted
 553 cystatins of the soft tick *Ornithodoros moubata*: differential expression pattern and inhibitory
 554 specificity. *Biological Chemistry* 387, 1635-1644.
- 555 Gulia-Nuss, M., Nuss, A.B., Meyer, J.M., Sonenshine, D.E., Roe, R.M., Waterhouse, R.M., Sattelle, D.B., de
 556 la Fuente, J., Ribeiro, J.M., Megy, K., Thimmapuram, J., Miller, J.R., Walenz, B.P., Koren, S., Hostetler,
 557 J.B., Thiagarajan, M., Joardar, V.S., Hannick, L.I., Bidwell, S., Hammond, M.P., Young, S., Zeng, Q.,
 558 Abrudan, J.L., Almeida, F.C., Ayllon, N., Bhide, K., Bissinger, B.W., Bonzon-Kulichenko, E.,
 559 Buckingham, S.D., Caffrey, D.R., Caimano, M.J., Croset, V., Driscoll, T., Gilbert, D., Gillespie, J.J.,
 560 Giraldo-Calderon, G.I., Grabowski, J.M., Jiang, D., Khalil, S.M., Kim, D., Kocan, K.M., Koci, J., Kuhn,
 561 R.J., Kurtti, T.J., Lees, K., Lang, E.G., Kennedy, R.C., Kwon, H., Perera, R., Qi, Y., Radolf, J.D.,
 562 Sakamoto, J.M., Sanchez-Gracia, A., Severo, M.S., Silverman, N., Simo, L., Tojo, M., Tornador, C., Van
 563 Zee, J.P., Vazquez, J., Vieira, F.G., Villar, M., Wespiser, A.R., Yang, Y., Zhu, J., Arensburger, P.,
 564 Pietrantonio, P.V., Barker, S.C., Shao, R., Zdobnov, E.M., Hauser, F., Grimmelikhuijzen, C.J., Park, Y.,
 565 Rozas, J., Benton, R., Pedra, J.H., Nelson, D.R., Unger, M.F., Tubio, J.M., Tu, Z., Robertson, H.M.,
 566 Shumway, M., Sutton, G., Wortman, J.R., Lawson, D., Wikel, S.K., Nene, V.M., Fraser, C.M., Collins,
 567 F.H., Birren, B., Nelson, K.E., Caler, E., Hill, C.A., 2016. Genomic insights into the *Ixodes scapularis*
 568 tick vector of Lyme disease. *Nat Commun* 7, 10507.
- 569 Guneidy, R.A., Shahein, Y.E., Abouelella, A.M., Zaki, E.R., Hamed, R.R., 2014. Inhibition of the
 570 recombinant cattle tick *Rhipicephalus (Boophilus) annulatus* glutathione S-transferase. *Ticks Tick*
 571 *Borne Dis* 5, 528-536.
- 572 Habig, W.H., Pabst, M.J., Fleischner, G., Gatmaitan, Z., Arias, I.M., Jakoby, W.B., 1974. The identity of
 573 glutathione S-transferase B with ligandin, a major binding protein of liver. *Proceedings of the*
 574 *National Academy of Sciences* 71, 3879-3882.
- 575 Hajdušek, O., Sojka, D., Kopáček, P., Burešová, V., Franta, Z., Šauman, I., Winzerling, J., Grubhoffer, L.,
 576 2009. Knockdown of proteins involved in iron metabolism limits tick reproduction and development.
 577 *Proceedings of the National Academy of Sciences* 106, 1033-1038.
- 578 Harwaldt, P., Rahlfs, S., Becker, K., 2002. Glutathione S-transferase of the malarial parasite *Plasmodium*
 579 *falciparum*: Characterization of a potential drug target. *Biological Chemistry* 383, 821-830.
- 580 He, H., Chen, A.C., Davey, R.B., Ivie, G.W., George, J.E., 1999. Characterization and molecular cloning of a
 581 glutathione S-transferase gene from the tick, *Boophilus microplus* (Acari: Ixodidae). *Insect Biochem*
 582 *Mol Biol* 29, 737-743.
- 583 Jaffe, J.J., Lambert, R.A., 1986. Glutathione S-transferase in adult *Dirofilaria immitis* and *Brugia pahangi*.
 584 *Molecular and biochemical parasitology* 20, 199-206.
- 585 Kansanen, E., Kuosmanen, S.M., Leinonen, H., Levonen, A.L., 2013. The Keap1-Nrf2 pathway:
 586 Mechanisms of activation and dysregulation in cancer. *Redox Biol* 1, 45-49.
- 587 Katoh, K., Misawa, K., Kuma, K., Miyata, T., 2002. MAFFT: a novel method for rapid multiple sequence
 588 alignment based on fast Fourier transform. *Nucleic Acids Res* 30, 3059-3066.
- 589 Kearse, M., Moir, R., Wilson, A., Stones-Havas, S., Cheung, M., Sturrock, S., Buxton, S., Cooper, A.,
 590 Markowitz, S., Duran, C., Thierer, T., Ashton, B., Meintjes, P., Drummond, A., 2012. Geneious Basic:
 591 An integrated and extendable desktop software platform for the organization and analysis of
 592 sequence data. *Bioinformatics* 28, 1647-1649.
- 593 Kopacek, P., Zdychova, J., Yoshiga, T., Weise, C., Rudenko, N., Law, J.H., 2003. Molecular cloning,
 594 expression and isolation of ferritins from two tick species--*Ornithodoros moubata* and *Ixodes ricinus*.
 595 *Insect Biochem Mol Biol* 33, 103-113.
- 596 Kröber, T., Guerin, P.M., 2007. *In vitro* feeding assays for hard ticks. *Trends in Parasitology* 23, 445-449.
- 597 Lara, F.A., Lins, U., Paiva-Silva, G., Almeida, I.C., Braga, C.M., Miguens, F.C., Oliveira, P.L., Dansa-Petretski,
 598 M., 2003. A new intracellular pathway of haem detoxification in the midgut of the cattle tick

- 599 *Boophilus microplus*: aggregation inside a specialized organelle, the hemosome. J Exp Biol 206,
600 1707-1715.
- 601 Lara, F.A., Lins, U., Bechara, G.H., Oliveira, P.L., 2005. Tracing heme in a living cell: hemoglobin
602 degradation and heme traffic in digest cells of the cattle tick *Boophilus microplus*. J Exp Biol 208,
603 3093-3101.
- 604 Lara, F.A., Pohl, P.C., Gandara, A.C., Ferreira, J.d.S., Nascimento-Silva, M.C., Bechara, G.H., Sorgine,
605 M.H.F., Almeida, I.C., Vaz, I.d.S., Oliveira, P.L., 2015. ATP Binding Cassette Transporter Mediates
606 Both Heme and Pesticide Detoxification in Tick Midgut Cells. PLoS One 10, e0134779.
- 607 Liebau, E., Bergmann, B., Campbell, A.M., Teesdale-Spittle, P., Brophy, P.M., Luersen, K., Walter, R.D.,
608 2002. The glutathione S-transferase from *Plasmodium falciparum*. Molecular and biochemical
609 parasitology 124, 85-90.
- 610 Liebau, E., De Maria, F., Burmeister, C., Perbandt, M., Turella, P., Antonini, G., Federici, G., Giansanti, F.,
611 Stella, L., Lo Bello, M., Caccuri, A.M., Ricci, G., 2005. Cooperativity and pseudo-cooperativity in the
612 glutathione S-transferase from *Plasmodium falciparum*. J Biol Chem 280, 26121-26128.
- 613 Liebau, E., Dawood, K.F., Fabrini, R., Fischer-Riepe, L., Perbandt, M., Stella, L., Pedersen, J.Z., Bocedi, A.,
614 Petrarca, P., Federici, G., Ricci, G., 2009. Tetramerization and cooperativity in *Plasmodium*
615 *falciparum* glutathione S-transferase are mediated by atypic loop 113-119. J Biol Chem 284, 22133-
616 22139.
- 617 Lumjuan, N., Stevenson, B.J., Prapanthadara, L.A., Somboon, P., Brophy, P.M., Loftus, B.J., Severson,
618 D.W., Ranson, H., 2007. The *Aedes aegypti* glutathione transferase family. Insect Biochem Mol Biol
619 37, 1026-1035.
- 620 Mashiyama, S.T., Malabanan, M.M., Akiva, E., Bhosle, R., Branch, M.C., Hillerich, B., Jagessar, K., Kim, J.,
621 Patskovsky, Y., Seidel, R.D., Stead, M., Toro, R., Vetting, M.W., Almo, S.C., Armstrong, R.N., Babbitt,
622 P.C., 2014. Large-Scale Determination of Sequence, Structure, and Function Relationships in
623 Cytosolic Glutathione Transferases across the Biosphere. Plos Biology 12.
- 624 Morphew, R.M., Eccleston, N., Wilkinson, T.J., McGarry, J., Perally, S., Prescott, M., Ward, D., Williams,
625 D., Raman, S.P.M., Ravikumar, G., Saifullah, M.K., Abidi, S.M.A., McVeigh, P., Maule, A.G., Brophy,
626 P.M., LaCourse, E.J., 2012. Proteomics and in Silico Approaches To Extend Understanding of the
627 Glutathione Transferase Superfamily of the Tropical Liver Fluke *Fasciola gigantica*. Journal of
628 Proteome Research 11, 5876-5889.
- 629 Morphew, R.M., MacKintosh, N., Harta, E.H., Prescott, M., LaCourse, E.J., Brophy, P.M., 2014. In vitro
630 biomarker discovery in the parasitic flatworm *Fasciola hepatica* for monitoring chemotherapeutic
631 treatment. EuPA Open Proteomics 3, 85-99.
- 632 Muller, S., 2015. Role and Regulation of Glutathione Metabolism in *Plasmodium falciparum*. Molecules
633 20, 10511-10534.
- 634 Nare, B., Smith, J.M., Prichard, R.K., 1992. Mechanisms of inactivation of *Schistosoma mansoni* and
635 mammalian glutathione S-transferase activity by the antischistosomal drug oltipraz. Biochemical
636 Pharmacology 43, 1345-1351.
- 637 Parizi, L.F., Utiumi, K.U., Imamura, S., Onuma, M., Ohashi, K., Masuda, A., Vaz, I.D., 2011. Cross immunity
638 with *Haemaphysalis longicornis* glutathione S-transferase reduces an experimental *Rhipicephalus*
639 (*Boophilus*) *microplus* infestation. Experimental Parasitology 127, 113-118.
- 640 Perally, S., Lacourse, E.J., Campbell, A.M., Brophy, P.M., 2008. Heme transport and detoxification in
641 nematodes: subproteomics evidence of differential role of glutathione transferases. Journal of
642 Proteome Research 7, 4557-4565.
- 643 Perner, J., Sobotka, R., Šíma, R., Konvičková, J., Sojka, D., Oliveira, P.L.d., Hajdušek, O., Kopáček, P.,
644 2016a. Acquisition of exogenous haem is essential for tick reproduction. eLife 5, e12318.
- 645 Perner, J., Provazník, J., Schrenková, J., Urbanová, V., Ribeiro, J.M.C., Kopáček, P., 2016b. RNA-seq
646 analyses of the midgut from blood- and serum-fed *Ixodes ricinus* ticks. Scientific Reports 6, 36695.

- 647 Pfaffl, M.W., 2001. A new mathematical model for relative quantification in real-time RT-PCR. *Nucleic*
648 *Acids Res* 29, e45.
- 649 Reddy, B.P., Prasad, G.B., Raghavendra, K., 2011. In silico analysis of glutathione S-transferase supergene
650 family revealed hitherto unreported insect specific delta- and epsilon-GSTs and mammalian specific
651 mu-GSTs in *Ixodes scapularis* (Acari: Ixodidae). *Comput Biol Chem* 35, 114-120.
- 652 Ricciardi, A., Ndao, M., 2015. Still hope for schistosomiasis vaccine. *Hum Vaccin Immunother* 11, 2504-
653 2508.
- 654 Ronquist, F., Huelsenbeck, J.P., 2003. MrBayes 3: Bayesian phylogenetic inference under mixed models.
655 *Bioinformatics* 19, 1572-1574.
- 656 Rosa de Lima, M.F., Sanchez Ferreira, C.A., Joaquim de Freitas, D.R., Valenzuela, J.G., Masuda, A., 2002.
657 Cloning and partial characterization of a *Boophilus microplus* (Acari: Ixodidae) glutathione S-
658 transferase. *Insect Biochem Mol Biol* 32, 747-754.
- 659 Sabadin, G.A., Parizi, L.F., Kio, I., Xavier, M.A., da Silva Matos, R., Camargo-Mathias, M.I., Githaka, N.W.,
660 Nene, V., da Silva Vaz, I., Jr., 2017. Effect of recombinant glutathione S-transferase as vaccine
661 antigen against *Rhipicephalus appendiculatus* and *Rhipicephalus sanguineus* infestation. *Vaccine* 35,
662 6649-6656.
- 663 Shahein, Y., Aboueilla, A., Hamed, R., 2013. Glutathione S-Transferase Genes from Ticks, in: Baptista,
664 G.R. (Ed.), *An Integrated View of the Molecular Recognition and Toxinology - From Analytical*
665 *Procedures to Biomedical Applications*. InTECH Open, pp. 267-289.
- 666 Shahein, Y.E., El Sayed El-Hakim, A., Aboueilla, A.M., Hamed, R.R., Allam, S.A., Farid, N.M., 2008.
667 Molecular cloning, expression and characterization of a functional GSTmu class from the cattle tick
668 *Boophilus annulatus*. *Vet Parasitol* 152, 116-126.
- 669 Sojka, D., Franta, Z., Horn, M., Caffrey, C.R., Mareš, M., Kopáček, P., 2013. New insights into the
670 machinery of blood digestion by ticks. *Trends in Parasitology* 29, 276-285.
- 671 Sonenshine, D.E., Roe, R.M., 2014. *Biology of ticks*, 2 ed. Oxford University Press.
- 672 Stamatakis, A., 2006. RAxML-VI-HPC: Maximum likelihood-based phylogenetic analyses with thousands
673 of taxa and mixed models. *Bioinformatics* 22, 2688-2690.
- 674 Swofford, D.L., 2003. *Phylogenetic Analysis Using Parsimony (*and Other Methods)*. Version 4. . Sinauer
675 Associates, Sunderland, Massachusetts.
- 676 Torres-Rivera, A., Landa, A., 2008. Glutathione transferases from parasites: a biochemical view. *Acta Trop*
677 105, 99-112.
- 678 Townsend, D.M., Tew, K.D., 2003. The role of glutathione-S-transferase in anti-cancer drug resistance.
679 *Oncogene* 22, 7369-7375.
- 680 van Rossum, A.J., Jefferies, J.R., Rijsewijk, F.A.M., LaCourse, E.J., Teesdale-Spittle, P., Barrett, J., Tait, A.,
681 Brophy, P.M., 2004. Binding of Hematin by a New Class of Glutathione Transferase from the Blood-
682 Feeding Parasitic Nematode *Haemonchus contortus*. *Infection and Immunity* 72, 2780-2790.
- 683 Vaz, I.D., Lermen, T.T., Michelon, A., Ferreira, C.A.S., de Freitas, D.R.J., Termignoni, C., Masuda, A., 2004a.
684 Effect of acaricides on the activity of a *Boophilus microplus* glutathione S-transferase. *Vet Parasitol*
685 119, 237-245.
- 686 Vaz, I.D., Imamura, S., Ohashi, K., Onuma, M., 2004b. Cloning, expression and partial characterization of
687 a *Haemaphysalis longicornis* and a *Rhipicephalus appendiculatus* glutathione S-transferase. *Insect*
688 *Molecular Biology* 13, 329-335.
- 689 Walker, J., Crowley, P., Moreman, A.D., Barrett, J., 1993. Biochemical properties of cloned glutathione S-
690 transferases from *Schistosoma mansoni* and *Schistosoma japonicum*. *Mol Biochem Parasitol* 61,
691 255-264.
- 692 Wei, J., Damania, A., Gao, X., Liu, Z., Mejia, R., Mitreva, M., Strych, U., Bottazzi, M.E., Hotez, P.J., Zhan, B.,
693 2016. The hookworm *Ancylostoma ceylanicum* intestinal transcriptome provides a platform for
694 selecting drug and vaccine candidates. *Parasit Vectors* 9.

- 695 Wilce, M.C.J., Parker, M.W., 1994. Structure and Function of Glutathione S-Transferases. *Biochimica Et*
 696 *Biophysica Acta-Protein Structure and Molecular Enzymology* 1205, 1-18.
- 697 Zhan, B., Liu, S., Perally, S., Xue, J., Fujiwara, R., Brophy, P., Xiao, S., Liu, Y., Feng, J., Williamson, A., Wang,
 698 Y., Bueno, L.L., Mendez, S., Goud, G., Bethony, J.M., Hawdon, J.M., Loukas, A., Jones, K., Hotez, P.J.,
 699 2005. Biochemical Characterization and Vaccine Potential of a Heme-Binding Glutathione
 700 Transferase from the Adult Hookworm *Ancylostoma caninum*. *Infection and Immunity* 73, 6903-
 701 6911.
- 702 Zhan, B., Perally, S., Brophy, P.M., Xue, J., Goud, G., Liu, S., Deumic, V., de Oliveira, L.M., Bethony, J.,
 703 Bottazzi, M.E., Jiang, D., Gillespie, P., Xiao, S.h., Gupta, R., Loukas, A., Ranjit, N., Lustigman, S.,
 704 Oksov, Y., Hotez, P., 2010. Molecular Cloning, Biochemical Characterization, and Partial Protective
 705 Immunity of the Heme-Binding Glutathione S-Transferases from the Human Hookworm *Necator*
 706 *americanus*. *Infection and Immunity* 78, 1552-1563.

707

708 **Legends to the Figures**

709

710 **Fig 1. Phylogeny and multiple alignment of selected chelicerate delta-/epsilon-class GST**
 711 **homologues. (A)** Maximum likelihood phylogenetic tree of delta-/epsilon-class GST homologues in
 712 chelicerates with *IrGST1* and its tick orthologues grouping in one well-supported clade. Nodal supports are
 713 shown for maximum likelihood and maximum parsimony bootstraps and Bayesian inference posterior
 714 probability. Sequences used for multiple amino-acid alignment in Fig. 1B are shown in bold **(B)** Multiple
 715 amino-acid alignment of *IrGST1* sequence with putative orthologues from other ticks and selected delta-
 716 /epsilon-class GSTs from other chelicerates. **Hard ticks:** *I. ricinus* - *IrGST1* (this work, GenBank
 717 MF984398); *I. scapularis* - *IsGSTD2* (GenBank XM_002436245); *I. persulcatus* (GenBank
 718 GBXQ01020781); *R. appendiculatus* (GenBank GEDV01003209); *R. microplus* (GenBank
 719 GEFA01011362); *A. aureolatum* (GenBank GFAC01002707); *D. variabilis* *DvGST1* (GenBank
 720 AY241958). **Soft ticks:** *O. moubata* (GenBank GFJQ02000585); *C. mimon* (GenBank GEIB01001162).
 721 **Mites:** *D. gallinae* (GenBank KR337506); *G. occidentalis* (GenBank XM_003746739); *T. urticae*
 722 (GenBank XM_015936065); *S. scabiei* (GenBank AY649788); *V. destructor* (GenBank
 723 XP_022657236). **Horseshoe crab:** *L. polyphemus* (GenBank XM_013931267). The hash symbol points to
 724 the conserved tyrosine residue of Y-type GSTs. The asterisks and dashed red frame depict the conserved
 725 GSTs signature motif of *IrGST1* orthologues as SRAI(A/G). The column next to the sequences shows
 726 sequence identity percentage related to *IrGST1*.

727

728 **Fig. 2. Analysis of *ir-gst1* expression by RT-qPCR and *IrGST1* levels by Western blotting. (A, B)**
 729 Analysis of midguts of ticks fed serum for 5 days (S), serum supplemented with haemin solvent (S-mock),
 730 625 μ M haemin (S+hm), 1% haemoglobin (equimolar to 625 μ M haemin) (S+Hb), or reconstituted blood

731 with 50% haematocrit (whole blood, WB). (A) RT-qPCR expression data are normalised against
 732 *elongation factor 1 α* (*ef1 α*). Shown data represent mean and SEM from three biological replicates. (B)
 733 Tick midgut homogenates were separated using reducing SDS-PAGE. Western Blot analysis was
 734 performed using specific rabbit anti-serum raised against *IrGST1* (*α IrGST1*) diluted 1:5000. (C) Midgut
 735 homogenates of ticks fed, for five days, serum supplemented with increasing haemin concentration were
 736 separated on reducing SDS-PAGE and Western Blot analysis was performed using *α IrGST1* (1:5000). (D)
 737 Midgut homogenates of seven days fed ticks, five days fed serum and for two consecutive days fed serum
 738 supplemented with 3 mg/ml bovine holo-Transferrin (Tf) or 10 mg/ml bovine Haemoglobin (Hb), were
 739 separated on reducing SDS-PAGE and Western Blot analysis was performed using *α IrGST1* (1:5000) and
 740 *α IrFer1* (1:50)

741
 742 **Fig. 3. RNAi verification and phenotypisation.** Adult *I. ricinus* ticks were injected with *ir-gst1* or *gfp*
 743 (control) dsRNA and allowed to recover for 24 hours (Day 0). Ticks (n = 25) were then placed on a rabbit
 744 and allowed to feed naturally for indicated time-points (Day 3, Day 5, and Day 7), then forcibly removed,
 745 weighed out, and their midguts dissected (n \geq 3). The remaining ticks were allowed to feed until repletion.
 746 (A) Tick midgut homogenates were separated by reducing SDS-PAGE and *IrGST1* protein levels were
 747 analysed by Western blotting using *α IrGST1* antibody (1:5000). (B) Sections were prepared from guts
 748 dissected from semi-engorged *I. ricinus* females (5 days of feeding). Section were labelled with *α IrGST1*
 749 serum (1:100) and Alexa488-conjugated anti-mouse antibody (left). DAPI was used to counterstain the
 750 nuclei. Sections were also stained with toluidine blue (right) - general structure of the tick gut showing the
 751 boundary between the gut epithelium and the gut lumen, containing large haemoglobin crystals (Hb) and
 752 developed digest gut cells (dGC); Nc - nuclei. (C) Column graph of tick weights before feeding and from
 753 individual time-points of feeding. Mean and SEM are shown, n \geq 3. (D) Oviposition and larvae hatching
 754 from fully engorged females upon RNAi.

755
 756 **Fig. 4. Purification of recombinant *IrGST1*, substrate profiling, and haemin inhibition assay.** (A)
 757 Soluble recombinant (His)₆-tagged *IrGST1* was purified from the lysate of expressing *E. coli* using Ni²⁺-
 758 IMAC under native conditions and fractions were analysed by reducing SDS-PAGE. Crude – *E. coli*
 759 lysate; Flow-through – unbound proteins; Elution – *IrGST1* eluted with 200 mM imidazole. (B) *IrGST1*
 760 from *I. ricinus* was tested for specific activities in spectrophotometric assays using GST model substrates;
 761 recombinant GST from *Fasciola gigantica* was used as a positive control (Morphew et al., 2012); 1-
 762 chloro-2,4-dinitrobenzene (CDNB) was used to test GSH-conjugation activity, trans 2-nonenal (T2N) was
 763 used to test GST-mediated reactions with reactive carbonyls, cumene hydroperoxide (C-HPx) was used to
 764 test peroxidase activity (C) Inhibition assays of haemin on CDNB activity of *IrGST1* and *F. gigantica*

765 over a range of different CDNB concentrations. **(D)** Dixon plot of inhibitory properties of haemin on
 766 *IrGST1* activity under different substrate (CDNB) concentrations. Calculated inhibitory constant (K_i) is
 767 shown. **(E)** CDNB assays testing inhibitory properties of haemin, haematin, protoporphyrin IX (PPIX),
 768 and myoglobin in a dilution series. **(B, D, E)** Mean and SEM from three independent measurements are
 769 shown.

770
 771 **Fig. 5. Assessment of haemin binding to *IrGST1* by haemin-agarose pull down and by VIS-**
 772 **spectrophotometry** **(A)** SDS-PAGE of the crude *E. coli* homogenate fractionated by haemin-agarose
 773 affinity absorption. Induced homogenate of *E. coli* expressing *IrGST1* was subjected to affinity pull-down
 774 by incubating the homogenate with haemin-agarose beads. Red asterisk indicates the protein band eluted
 775 with 1 M urea and submitted for mass-fingerprint identification. CDNB activities (nmol CDNB/min/mg
 776 protein) of individual fractions are shown below the gel picture, mean \pm SEM from three measurements.
 777 Activity of eluted fraction was not determined due to the presence denaturing urea in elution buffer. **(B)**
 778 Titration of *IrGST1* was carried out in a range of molar ratios to the constant concentration of 10 μ M
 779 haemin. **(C)** A plot of absorbance values at 421 nm in relation to molar ratios of *IrGST1* and haemin.

780
 781 **Fig. 6. Purification and haem-binding of untagged *IrGST1*.** **(A)** SDS-PAGE monitoring a two-step
 782 purification of untagged *IrGST1* from *E. coli* homogenate (Crude). First step was performed by anion
 783 exchange (IEX) chromatography using MonoQ column. Second step was performed by size-exclusion
 784 chromatography (SEC) using Superdex 75 column. **(B)** SEC chromatogram of purified untagged *IrGST1*
 785 detected at 280 (black line) and 400 nm (red line). The elution volumes of molecular weight standards are
 786 indicated by arrows. The deduced molecular weight of *IrGST1* was calculated using a logarithmic
 787 standard curve. **(C)** SEC chromatogram detecting both 280 nm (black line) and 400 nm (red lines) of
 788 purified *IrGST1* pre-incubated with varying molar ratios of haemin.

789

790 **Legends to the Supplementary Figures**

791
 792 **Supplementary Fig. S1. Multiple amino acid alignment of *IrGST1* sequence with putative**
 793 **homologues of delta-/epsilon-class GSTs from *I. scapularis* genome.** *IrGST1* (*Ixodes ricinus*, this work,
 794 GenBank MF984398); Right panel table – Nomenclature, VectorBase and GenBank accession Nos of *I.*
 795 *scapularis* genes encoding delta-/epsilon-class GSTs adopted from (Reddy et al., 2011).

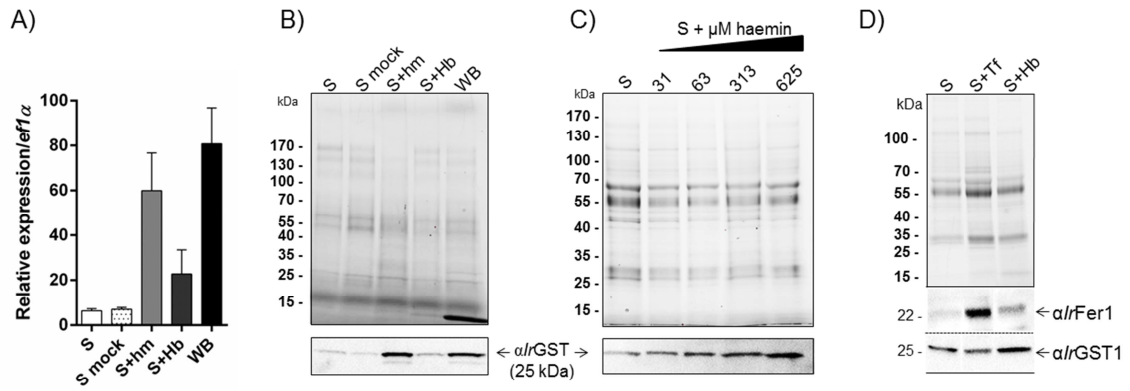
796
 797 **Supplementary Fig. S2. Immunohistochemistry evaluation of lipid peroxidation.** Sections were
 798 prepared from guts dissected from semi-engorged *I. ricinus* females (5 days of feeding). Section were

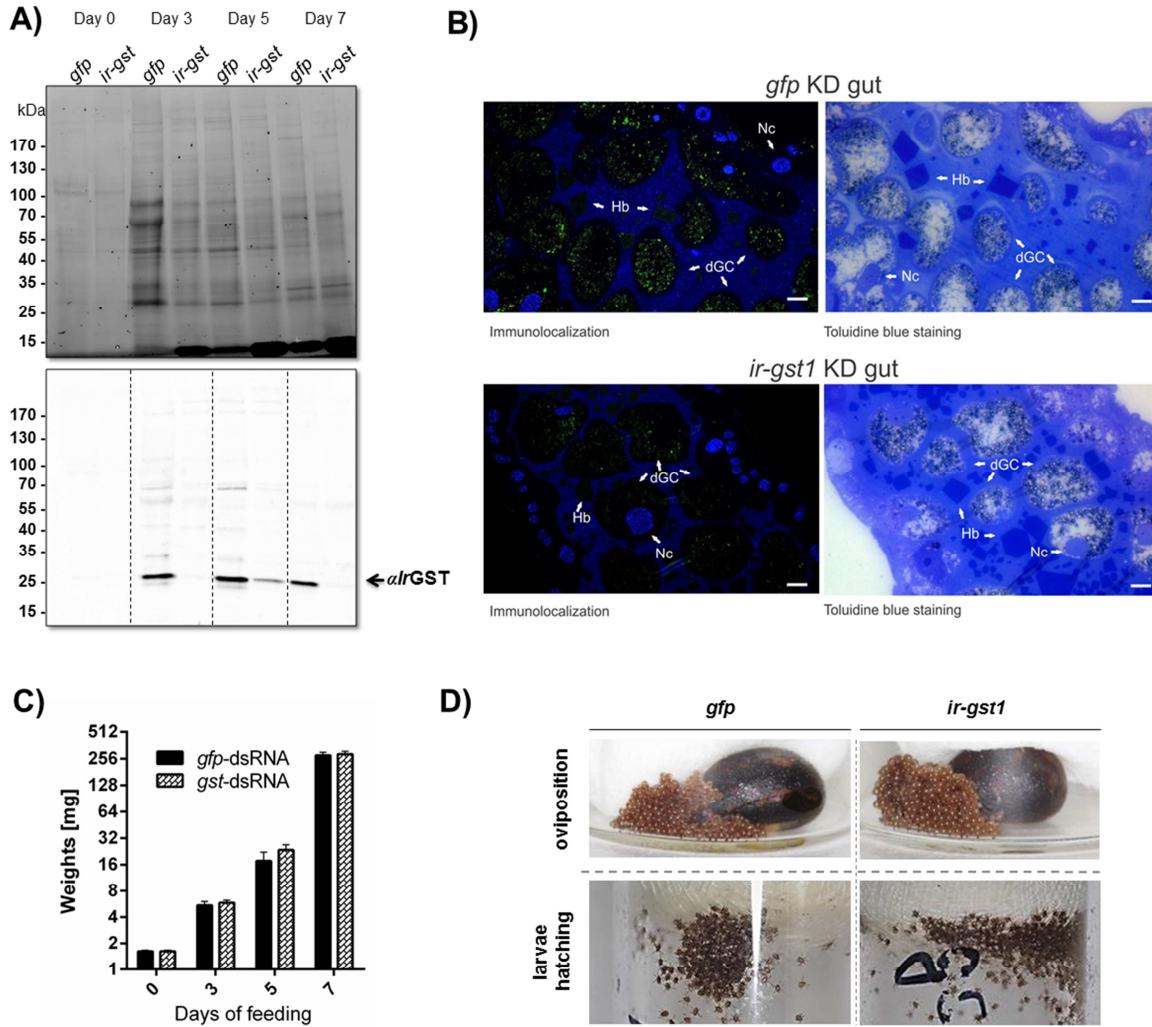
799 labelled with rabbit α 4-HNE (1:300) and Alexa488-conjugated anti-rabbit antibody (left). DAPI was used
800 a counterstain. Sections were also stained with toluidine blue (right) - general structure of the tick gut
801 showing the boundary between the gut epithelium and the gut lumen, containing large haemoglobin
802 crystals (Hb) and digest gut cells (dGC); Nc - nuclei.

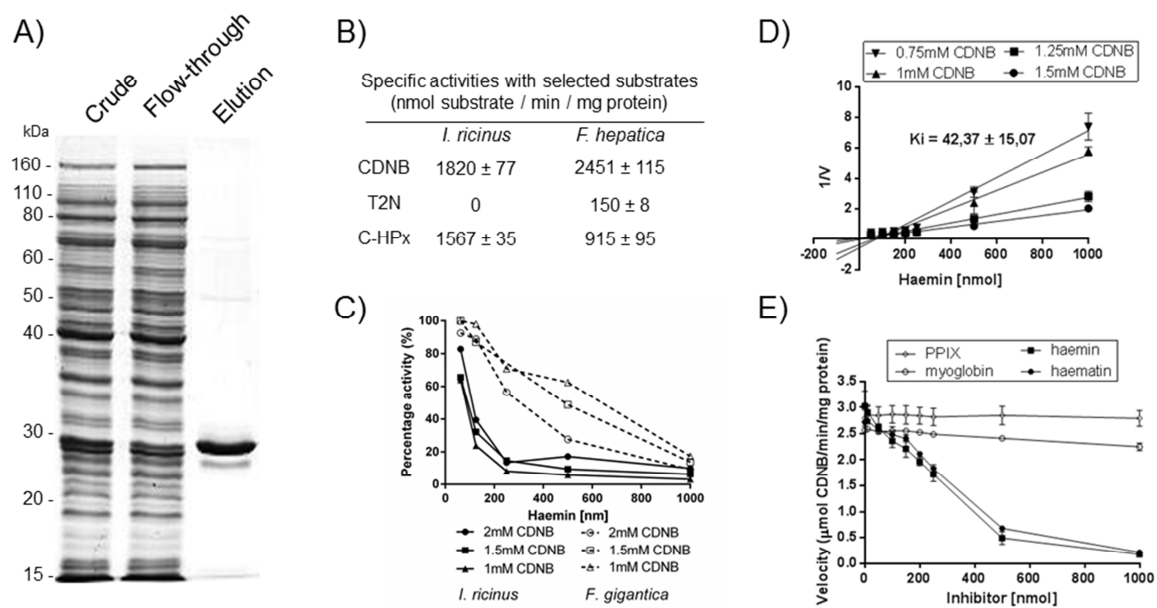
803
804 **Supplementary Fig. S3. Binding of *IrGST1* to glutathione or S-hexyl glutathione agarose.** (A)
805 Activity measurements with titrated 1-chloro-2,4-dinitrobenzene (CDNB) concentrations to calculate
806 Michaelis-Menten constant (K_m). (B) Activity measurements with titrated glutathione (GSH)
807 concentrations to calculate Michaelis-Menten constant (K_m). (C) Induced *E. coli* fraction as well as Ni^{2+} -
808 IMAC purified *IrGST1* were subjected to glutathione or S-hexyl glutathione (S6) agarose. Individual
809 fractions were examined by SDS-PAGE and activity measurements. Mean and SEM are shown, $n = 3$. FT
810 - flow-through, E - elution, N.D. - not determined with a given detection limit.

811
812 **Supplementary Fig. S4. Isoelectric focusing electrophoresis of purified untagged *IrGST1*.** Standard
813 pI values of the markers (M) are indicated on the left.

814
815 **Supplementary Fig. S5. Haem-binding size exclusion chromatography (SEC).** SEC chromatogram
816 detecting both 280 and 400 nm of purified untagged *IrGST1* pre-incubated with varying molar ratios of
817 haemin. Arrows point towards a deduced dimeric form of the protein, asterisks denote a higher molecular
818 weight *IrGST1*:haemin complex as a potential polymer.

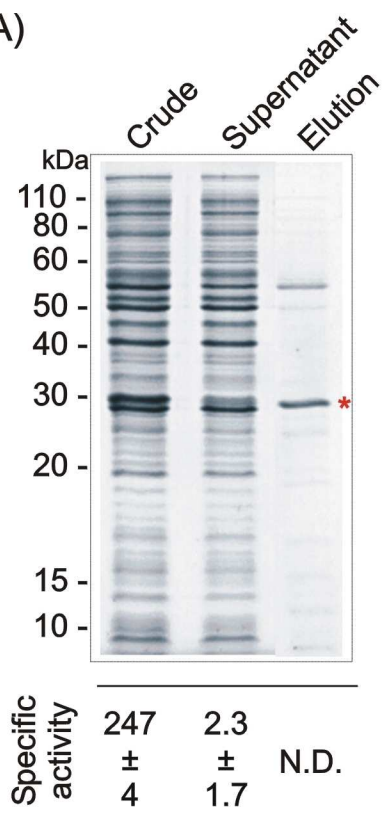




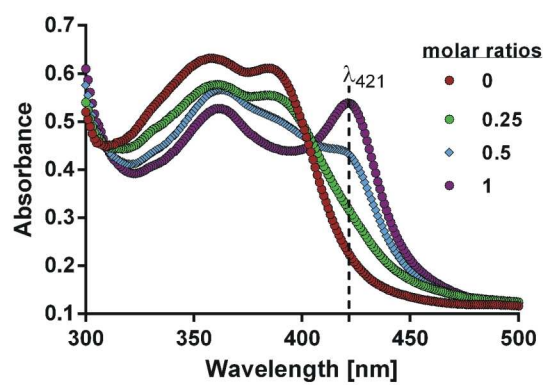


ACCEPTED MANUSCRIPT

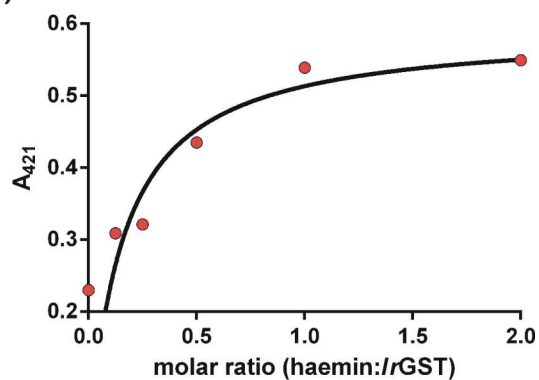
A)

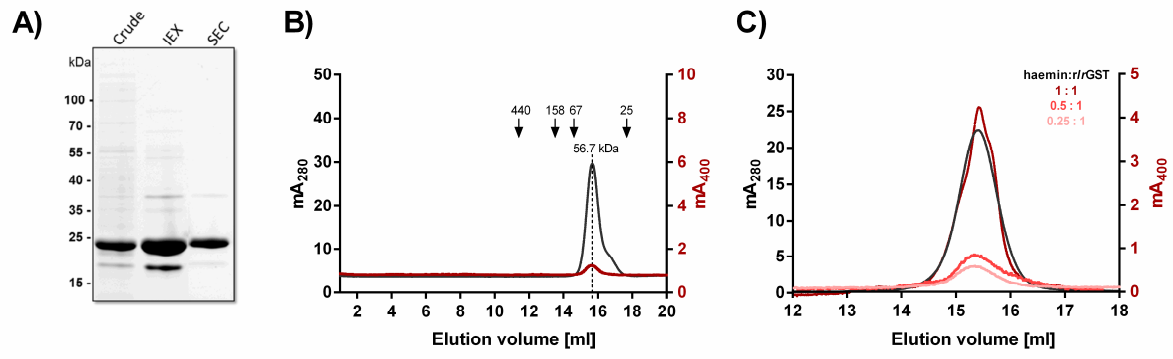


B)



C)





Highlights

- Haem-inducible *IrGST1* from *Ixodes ricinus* is the first functionally characterised tick GST of delta-/epsilon-class
- *IrGST1* and its orthologues from other ticks form a phylogenetically distinct clade of GSTs that secondarily acquired haem-binding properties
- *ir-gst1* tick gut expression is induced by host haem, but not by host iron
- *IrGST1* binds haemin *in vitro* and is presumably an endogenous intracellular scavenger of excessive haem